Ecological Engineering 103 (2017) 180–190

Contents lists available at ScienceDirect

Ecological Engineering

journal homepage: www.elsevier.com/locate/ecoleng

Green synthesis of zinc oxide nanoparticles using *Peganum harmala* seed extract, and loaded on *Peganum harmala* seed powdered activated carbon as new adsorbent for removal of Cr(VI) from aqueous solution

Mehdi Fazlzadeh[a,*], Rasoul Khosravi[b], Ahmad Zarei[c]

[a] PhD candidate, Member of Student Research Committee, Environmental Health Engineering, Shahid Sadoughi University of Medical Sciences, Yazd, Iran
[b] Environmental Health Engineering, School of Health, Gonabad University of Medical Sciences, Gonabad, Iran
[c] Department of Environmental Health Engineering, School of Health, Ardabil University of Medical Sciences, Ardabil, Iran

ARTICLE INFO

Article history:
Received 1 November 2016
Received in revised form 2 February 2017
Accepted 19 February 2017

Keywords:
Green synthesis
Adsorption
Cr(VI)
GZnO
Powdered activated carbon
Peganum harmala

ABSTRACT

In the present work, powdered activated carbon was derived from *Peganum harmala* seed (PPAC) and then coated by green ZnO nanoparticles and finally applied for Cr(VI) removal. PPAC was activated using a new physicochemical method in the presence of ultraviolet waves. FESEM showed that PPAC has a high structural porosity. Based on TEM, the size of synthesized NPs was 40 nm. Moreover, EDAX confirmed the existence of NPs on PPAC. FTIR spectrum showed the polyphenolic groups available in *Peganum harmala* seed extract in the synthesis of NPs. BET analysis presented a specific surface area of 442 m^2/g for PPAC which declined after GZnO coating. Experimental data showed that coating GZnO on PPAC enhance the sorption percentage of the adsorbent significantly. The optimum pH value was found to be 2. The overall adsorption efficiency increased with a rise in temperature. The thermodynamic data indicated that the adsorption process by the adsorbent was endothermic and spontaneous in nature. Furthermore, equilibrium data showed that Cr(VI) adsorption fitted well with pseudo second order kinetic model and the Langmuir isotherm model was found to describe the adsorption process better. The maximum adsorption capacity of GZnO/PPAC was found to be 74.67 mg/g.

1. Introduction

Chromium, as a toxic metal, is usually present in three and hexavalent states in aqueous solutions (Jing et al., 2014). Cr(III), trivalent, is the most stable and important oxidation state of chromium, relatively stable in the aquatic system due to its rather low water solubility, therefore, it does not create health hazards (Ahmad et al., 2011). It is critical to maintain and storage carbohydrate, protein, and fat in the body (Nethaji et al., 2013). Chromium (VI) is toxic and carcinogenic to humans. High exposure to Cr(VI) may cause nausea, vomiting, kidney and liver damage (Fazlzadeh et al., 2017; Jing et al., 2014; Nethaji et al., 2013). Dermal exposure with chromium can result in allergic responses, skin ulcers and skin necrosis (Bayat, 2002). Generally speaking, Cr(VI) is an indicator of contamination of water by human (Limei et al., 2013). Maximum acceptable concentration (MAC) of Cr(VI) in surface and drinking water is 0.1 mg/l and 0.05 mg/l, respectively. Effluents from industries, such as tannery, electroplating, dying, paper production, refineries and wood processing (Vinod et al., 2010; Zhongren et al., 2009) and steel (Bansal et al., 2009), contain significant quantities of Cr(VI). Therefore, it is necessary to remove chromium containing effluents before discharging them into the environment (Ahmad et al., 2011). A number of treatment techniques for the removal of Cr(VI) from aqueous environments have been reported, mainly membrane filtration, ion exchange, adsorption, electrochemical precipitation, reduction of Cr(VI) into Cr(III), reverse osmosis, evaporation, complexing, solvent extraction and electrolysis. However, most of the above mentioned techniques are quite inefficient due to low efficiency, high operational costs and investment, high amount of energy consumption, expensive treatment and disposal of generated sludge, which are not eco-friendly (Babak et al., 2014). Among these techniques, adsorption is an effective process that has advantages in terms of flexibility and design simplicity, cost, easy regeneration, and low amounts of biological and chemical sludge generation, and ease of operation

* Corresponding author.
E-mail addresses: m.fazlzadeh@gmail.com (M. Fazlzadeh), Khosravi.r89@gmail.com (R. Khosravi), m.fazlzadeh@gmail.com (A. Zarei).

http://dx.doi.org/10.1016/j.ecoleng.2017.02.052
0925-8574/

compared to other techniques (Agnieszka et al., 2011; Pirsaheb et al., 2014). Adsorption process is a mass transfer physical or chemical process in which pollutant molecules enter from bulk phase to solid material (Mahmood-ul-Hassan et al., 2015). Nowadays, the nanotechnology appears to be an attractive, reasonable, and promising option to solve the environmental issues caused by different industrial effluents. Nano-materials exhibit a number of special characteristics such as extremely small size, the absence of internal diffusion resistance and high surface area to volume ratio, relative to bulk material which provide better the adsorption efficiency of contaminants from aqueous environments (Mehrorang et al., 2013). Synthesis of nanoparticles (NPs) is an expensive process and requires specific separation techniques from aqueous solutions (Fazlzadeh et al., 2016). NPs are usually coated onto oxides, polymers, textiles and activated carbon. Among these, application of activated carbon has shown advantages from the economic and environmental consideration (Ghaedia et al., 2012; Mehrorang et al., 2013). Different physical and chemical methods (Shahwan et al., 2011) such as use of sodium borohydride (NaBH4), ethylene glycol, carbo-thermal synthesis, citric acid and chitosan have been applied for NPs synthesis (Prasad et al., 2014). The aggregation of these NPs in a linear form is one of their important characteristics, which generally reduce the surface area to volume ratio. Organic surfactants or capping agents can be used for the improvement of electrostatic repulsion among NPs (Prasad et al., 2014; Shahwan et al., 2011). Biological method of NPs generation using green synthesis has been receiving increased attention owing to their eco-friendly, nontoxic nature, and stability against agglomeration (Prasad et al., 2014; Weng et al., 2013). In this method, various plant extracts and products can be used as an alternative to chemical and physical synthesis of NPs (16). Recently, plant extracts including extract of black and green tea, oolong tea leaves, (Huang et al., 2014), grape residues, grape leaves, black tea (Machado et al., 2013), green tea and eucalyptus leaves (Wang et al., 2014) has been used for the synthesis of nZVI and other NPs. In the present study, the extract of *Peganum harmala* seed, an abundantly growing desert plant in south Khorasan province, Iran was efficiently used as a stabilizing agent for the preparation of ZnO nanoparticles (ZnO NPs). Then, the prepared NPs were coated on powdered activated carbon derived from *Peganum harmala* seeds by use of a novel method called floating method. In the present research, the powdered activated carbon was produced using ultrasonic waves without the application of steam and nitrogen.

2. Materials and methods

2.1. Preparation of powdered activated carbon (PPAC)

Granular seeds of *Peganum harmala* were collected from south Khorasan province. This plant grows in large numbers in desserts of Iran and many countries of Middle East, Asia and some parts of the United States of America. Until now, there is no an application for this plant in industry. It is sometimes being used in religious beliefs as protecting against “devil eye”. Preparation of one kilo of *Peganum harmala* costs 3–4 cents which is very cost effective.

After collection, the seeds were thoroughly washed several times with distilled water and ground well. The well-grounded material was sieved through a 60 mesh screen and, then it was impregnated with phosphoric acid 50% and dried for 48 h at room temperature (Liu et al., 2010). Afterwards, the dried material was placed in a cylindrical steel reactor. The reactor then was placed in a programmable furnace model, HL40P controller. Furnace temperature reached 800 °C at a rate of 5 °C per minute and then we remained it in this temperature for 2 min. After furnace cooling, *Peganum harmala* powdered carbon (PPC) was removed from the furnace. For activation, PPC was added in 3N HCl in a 500 ml beaker and then it was exposed to ultrasonic (model Elmasonic E 30H) at 37 KHz frequency for 1 h. Finally, the produced PPAC was washed two times with distillated water until its pH value reached 6. PPAC was then placed in an oven for 2 h at 110 °C to be dried completely. Finally, PPAC was stored in a dry place for further use.

2.2. Synthesis of ZnO nanoparticles (GZnO)

In this study, Powdered *Peganum harmala* seed (PPH) was used to synthesize ZnO NPs. PPH weighing 6 g was mixed with 100 ml distilled water and then transferred to 500 ml conical flask and the content was placed on a 300 rpm magnetic stirrer. The solution temperature on the mixer was fixed at 80 °C. After 1 h extracting, the mixture was removed from the magnetic heater, cooled and then filtered through a vacuum pump. The produced extract was mixed with zinc nitrate (4–1 ratio). After that, the solution was exposed to ultrasonic for 1 h. Synthesized NPs appeared with a white color. Then the mixture was poured into a graduated cylinder, washed 3 times with ethanol and then rinsed with double distilled water. Finally, the residue was placed into a 50 °C oven to be completely dried. The synthesized NPs were ground and stored for further use.

2.3. Coating ZnO NPs on powdered activated carbon (GZnO/PPAC)

After PPAC preparation and GZnO synthesis, 0.05 gr of GZnO was mixed into 200 ml distilled water and agitated for 10 min on a magnetic stirrer to obtain uniform distribution. Then, 5 gr activated carbon was added into the solution and placed again onto magnetic stirrer at 500 rpm for 10 h to complete coating process. After that, activated carbon was separated using a filter. The filtrate was then washed with double distilled water and placed in oven (95 °C) for 10 h to be completely dried.

2.4. Adsorbents characterization

TEM images were taken by a TEM model Philips CM30 operating at 120 keV. NPs samples were dispersed in methanol for 20 min. ZnO NPs and coated PPAC were characterized morphologically by doing FESEM. Moreover, the EDAX analysis was used to identify the presence of ZnO NPs coated on PPAC. These analyses were done using FESEM/EDAX model Mira 3-XMU. Specific surface area (BET) and total pore volume were obtained by adsorption **at250 °C on Belsorp mini II** (Bel, Inc. Japan). Finally, the functional groups on the adsorbent surface were determined by FTIR Spectrum RX I (PerkinElmer, USA).

2.5. Experimental

This experimental study was done on a batch manner in 100 ml conical flasks. Desired Cr(VI) concentrations were prepared from a 1000 mg/l stock solution of chromium. Initially, 50 ml of sample with a desired concentration was poured into conical flasks. The chromium stock was prepared from $K_2Cr_2O_7$. The pH of the chromium solutions was adjusted using 0.1 N NaOH and HCl. Then, certain adsorbent doses were added into the flasks and placed immediately onto shaker with a fixed agitation speed. After the contact time elapsed, the sample was filtered using a whatman paper No. 0.45 μm. Then, the filtered sample was analyzed for determination of chromium level. The effect of experimental parameters, namely, pH (2, 3, 4, 5, 6, 7, 8) and adsorbent dose (1, 2, 3, 4, 5, 6, 7, 8, 9, 10 g/l), contact time (5, 10, 15, 20, 30, 40, 60, 80 min), initial concentration (10, 25, 50, 75, 100 mg/l), agitation speed (0, 50, 100, 150, 200, 300 rpm) and temperature (10, 20, 30, 40, 50 °C) were

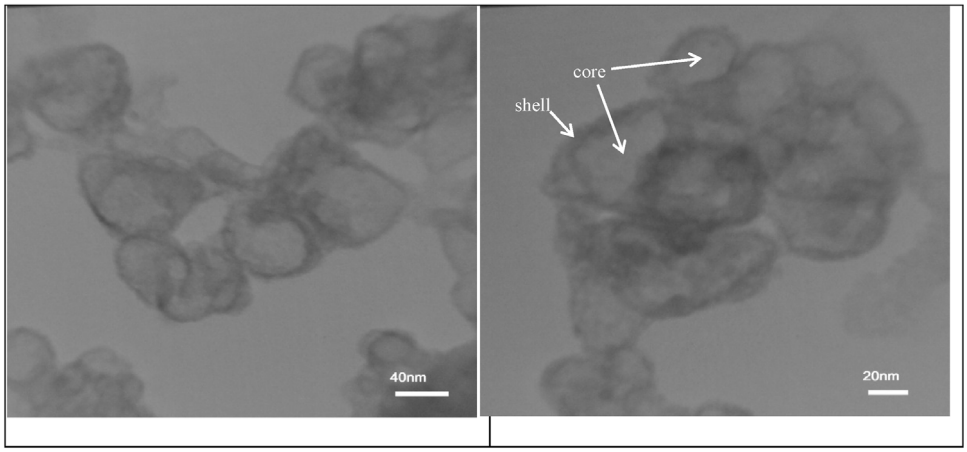

Fig. 1. TEM images of GZnO synthesized from extract of *Peganum harmala* seed.

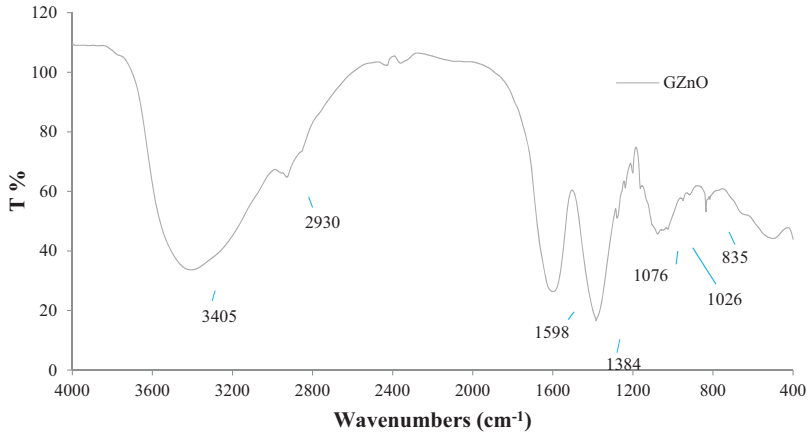

Fig. 2. FTIR spectrum depicting GZnO synthesized from *Peganum harmala* seed.

studied. All the experiments were performed in duplicate and the mean values were reported.

2.6. Determination of Cr(VI) concentration

The concentrations of chromium in the solutions were determined using UV/VIS Spectrophotometer T80+ at 540 nm according to the method described by Standard Methods for the Examination of Water and Wastewater (APHA, AWWA, WEF, 2005). All the reagents used were of analytical grade which were purchased from the MERK, Germany. All the experimental data was performed and analyzed using Excel software.

3. Results and discussion

3.1. Characterization of synthesized adsorbent

Transmission electron microscopy (TEM) was used to determine the size and size distribution of the NPs. Fig. 1 shows two images of GZnO using extract of *Peganum harmala* seed. The size of synthesized NPs was 40 nm with non-uniform shape. The images obviously show the successful synthesis of the NPs. Based on the images, synthesized NPs have two separate parts; the core and the shell. The core and the shell (with size of 2 nm) of NPs indicate GZnO and the capping and stabilizing materials available on plant extract, respectively. The crust protects the NPs against oxidation. The types of these compounds and their role in NPs synthesis can be determined better by FTIR analysis. A FTIR analysis in range of 400–4000 cm^{-1} (Fig. 2) was used to determine functional groups on GZnO. According to the figure, the FTIR spectra with absorption peaks at 835, 1026 & 1076, 1384, 1598, 2930, 3405 indicating C—H bending of aromatics, C—N stretching vibration of amine, CH_3 bending of alkanes, N—H bending of amines, O—H stretching of carboxylic acid, C—H stretching of alkanes, O—H stretching of polyphenols were observed. Polyphenols acts as the main stabilizing agents for NPs which can be seen at 3200–3500 cm^{-1}. It can be seen from the other peaks that GZnO NPs were surrounded by proteins and metabolites such as terpenoids and caffeine. Carbonyl groups corresponding to amino acid residue and proteins have a high affinity to bond with metal ions; stabilizing NPs and preventing their agglomeration (Ramesh et al., 2015). The existence of these compounds around the NPs is evident in TEM image. Moreover, the functional groups of activated carbon derived from *Peganum harmala* seeds before and also after coating are compared and the results are summarized in Fig. 3. Fig. 3(a) and (b) shows the PPAC and GZnO/PPAC, respectively. After coating GZnO on PPAC, strong peak at 3433 cm^{-1} was not changed but peak at 2360 cm^{-1} was disappeared completely. Furthermore, an additional peak was appeared at 2284 cm^{-1}. Some narrow peaks at 1868, 1708 and 1653 cm^{-1} were disappeared completely. Peaks at 1540, 1457 and 1171 cm^{-1} were shifted to 1596, 1440 and 1187 cm^{-1}, respectively. The peak at 502 cm^{-1} was also disappeared. Some small peaks disappeared after coating GZnO on PPAC and

irregularity of FTIR spectrum of GZnO/PPAC became less. The changes occurred at PPAC spectrum after coating on GZnO confirmed the formation of new functional groups and generally

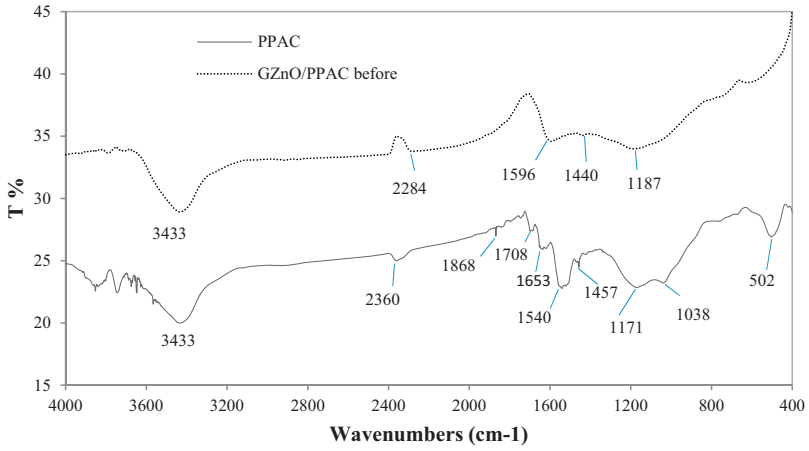

Fig. 3. FTIR spectra of PPAC and GZnO/PPAC.

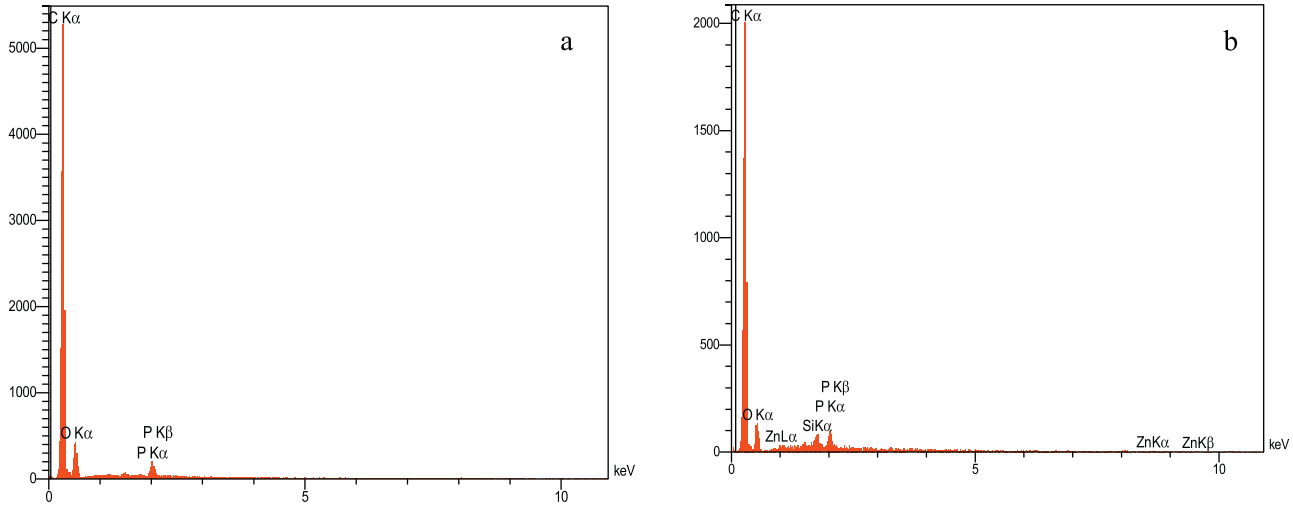

Fig. 4. EDX spectra showing (a) the absence of Zn ions on PPAC, and (b) Zn ions on GZnO/PPAC.

showed the successful coating of PPAC on GZnO. EDAX analysis (Fig. 4) was used to present the coating of NPs on PPAC. In Fig. 4(a), there are not any Zn ions on PPAC. But in Fig. 4(b) Zn ions are adsorbed on GZnO/PPAC. The results also confirm the FTIR analysis. FESEM was used to characterize adsorbents morphology. Fig. 5 depicts FESEM images of the adsorbents. According to Fig. 5 which shows GZnO image, we can see the irregular shapes of NPs. The size of NPs in the figure is the same as that in TEM image. Fig. 5(b) shows the surface of PPAC. A high porosity and uniform surface can be seen in the figure. In this image, the presence of many pores proves the important role of ultrasonic waves on carbon activation. Theses pores are declined in Fig. 5(c) that confirms the BET results. In the image, the surface of the adsorbent is not very porous as that of PPAC. This can be attributed to NPs coating on the surface of PPAC which in general decreases the porosity. Fig. 5(d) shows the morphology of GZnO/PPAC after Cr(VI) adsorption. It can be obviously seen in the figure that the number of irregularities declined on adsorbent surface due to formation a layer on the surface resulting from Cr(VI) adsorption. BET analysis was applied to evaluate specific surface area of activated carbon prepared by a new method using ultrasonic waves. Using the analysis, total pore volume and average pore size were determined. The surface area, pore volume and pore size of NPs were 442 m^2/g, 23.3×10^{-2} g/cm^3 and 2 nm, respectively based on BET analysis, which declined to 208 m^2/g and 9.76×10^{-2} g/cm^3 and 182 nm, respectively. The result show that the surface area of the adsorbent decreased after NPs coating. Therefore, it can be concluded that both chemical and physical adsorption took place in the adsorbent.

3.2. Effect of pH on Cr(VI) adsorption

The relation between the solution pH and the removal efficiency of Cr(VI) using GZnO and PPAC is shown in Fig. 6. The findings show that hexavalent chromium adsorption highly depends on pH value and maximum adsorption capacity occurred at acidic pHs. With increase in pH value, the adsorption capacity decreased. Accordingly, at pH = 2, the adsorption capacities of PPAC and GZnO/PPAC were 16.63 and 27.73 mg/g, respectively. While at pH = 8, the values significantly decreased to 0.67 and 1.55 mg/g, respectively.

Changes in Cr(VI) adsorption efficiencies with pH can be attributed to the availability of different forms of chromium. $HCrO^{4-}$ and Cr_2O^{7-} are the predominant forms of Cr(VI) at acidic pHs. But at basic solutions, $CrO_4{}^{2-}$ is the only stable form (Gottipati and Mishra, 2016; Khosravi et al., 2014). By decreasing pH value to the range of 2–6, the equilibrium shift to dichromate side (Gottipati and Mishra, 2016).

$$2CrO_4^{2-} + 2H^+ \rightarrow Cr_2O_7^- + H_2 \quad (1)$$

By rising pH value, the equation shifts to the left, so the level of chromate ($CrO_4{}^{2-}$) increases. Chromate ions due to having two

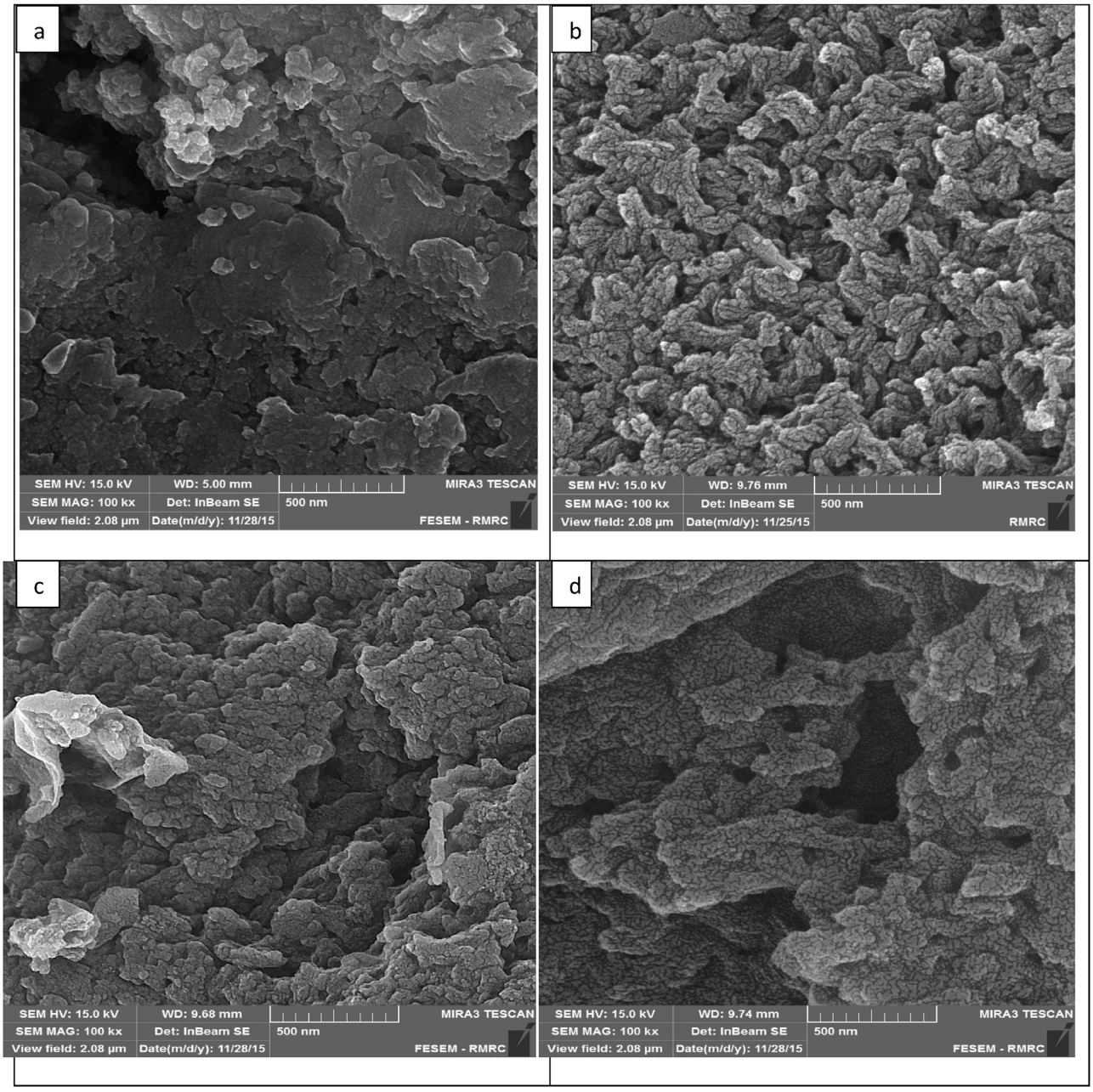

Fig. 5. SEM images of GZnO (a), PPAC (b), GZnO/PPAC before (c), and GZnO/PPAC after Cr(VI) adsorption (d).

minus charges requires two active site for efficient adsorption, whereas other forms of chrome which existing in acidic pHs, only need one active site (Yang et al., 2015). This causes that adsorption capacity of this adsorbent in the presence of CrO_4^{2-} anions and absence of any inhibiting agent be half of that in the presence of $HCrO^{4-}$ and Cr_2O^{7-}. Moreover, at low pHs, there is a high degree of protonation on adsorbent surface providing a good environment for reaction of active sites and Cr(VI) in anionic form, thus increasing the electrostatic attraction, whereas at high pHs there is a fall in the degree of protonation as competition between OH^- and CrO_4^{2-} ions which lead to successful occupation of the active surface sites by OH^- ions, thus, reducing the overall uptake capacity (Gopalakannan et al., 2016; Gottipati and Mishra, 2016). The result of pH influence on Cr(VI) removal in the present study is consistent with the results reported by the previous studies (Zhang et al., 2015; Yang et al., 2015). According to the results presented in Fig. 7, it is obvious that the adsorption capacity of PPAC has increased significantly after coating GZnO on PPAC. For example, at pH = 2, adsorption capacity of the adsorbent has increased by 1.7. However, the increase in adsorption capacity occurred when specific surface area of GZnO/PPAC was half of that of PPAC. Based on the result, it can be stated that GZnO synthesis from *Peganum harmala* seed enhanced the removal potential of Cr(VI). This can be attributed to the increase in the number of sharing electrons between GZnO and Cr(VI). This finding was also obvious in thermodynamic study.

3.3. *Effect of adsorbent dosage on Cr (VI) adsorption*

Based on Fig. 7, adsorption capacity decreases significantly with increase in adsorbent dosage. Accordingly, at a dose 0.5 g/l, the adsorption capacity of GZnO/PPAC was 68.38 mg/g and with increase of dosage to 10 g/l, the adsorption capacity reached to 5.73 mg/g. By increasing adsorbent dosage from 0.5 to 2, the removal efficiency changed from 59.65% to 97.59%. At higher

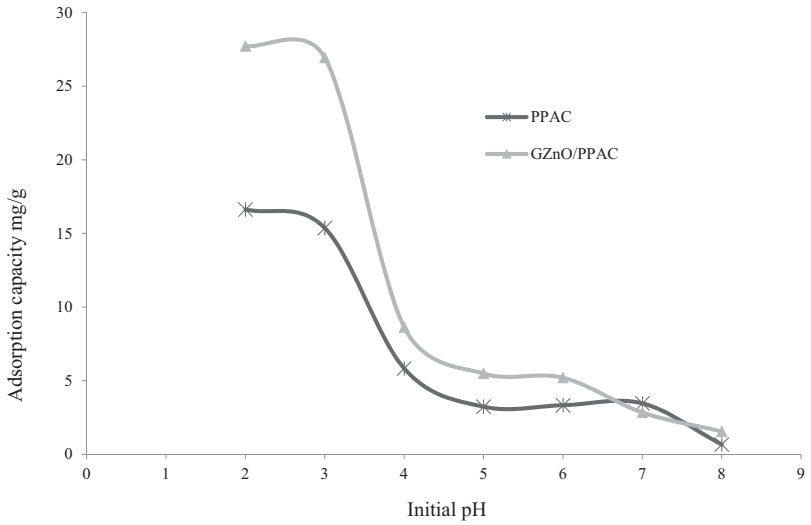

Fig. 6. Effect of pH (adsorbent dose = 2 g/l, contact time = 30 min, Cr(VI) concentration = 50 mg/l, agitation speed = 200 rpm).

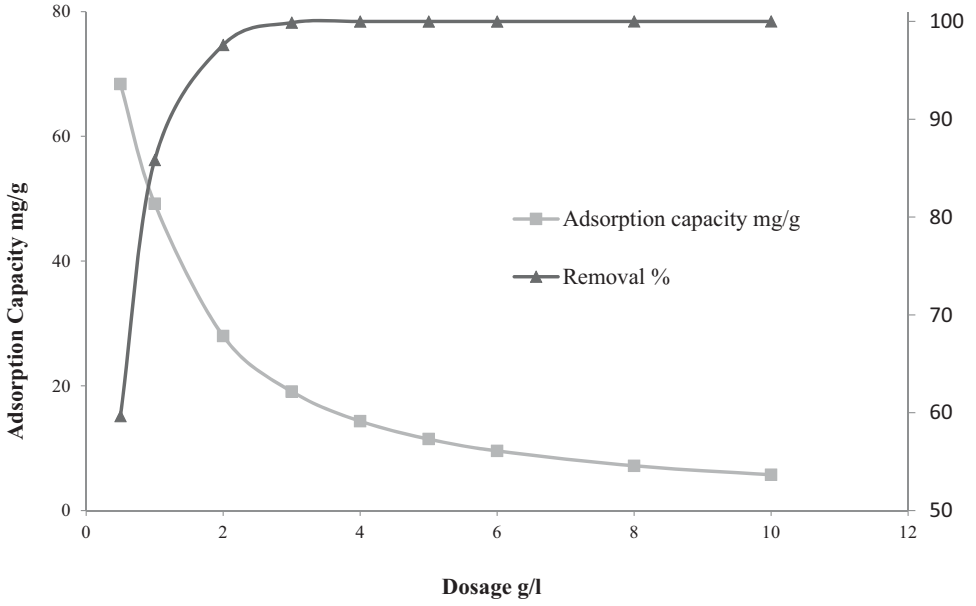

Fig. 7. Effect of adsorbent dose (contact time = 30 min, Cr(VI) concentration = 50 mg/l, adsorbent dose = 2 g/l, agitation speed = 200 rpm, pH = 2).

dosages (>2 g/l), a steady behavior occurred and therefore, no significant change in removal efficiency occurred. Removal percentage increased with increasing adsorbent dosage. Inversely, with increase in adsorbent dosage, the adsorption capacity decreased due to the availability of more surfaces and hence, active sites for Cr(VI) adsorption. At the beginning, the Cr(VI) removal percentage increased rapidly with increasing adsorbent dosage, and then, the rate was slower; finally, a plateau was reached (6). In the present study, 2 g/l adsorbent dosage was found to be optimum which is an ideal value considering high removal efficiency and also economic aspects. Similar findings have been reported for the removal of different pollutants in scientific literature (Granados-Correa and Jiménez-Becerril, 2009; Jung et al., 2013; Moussavi and Khosravi, 2011).

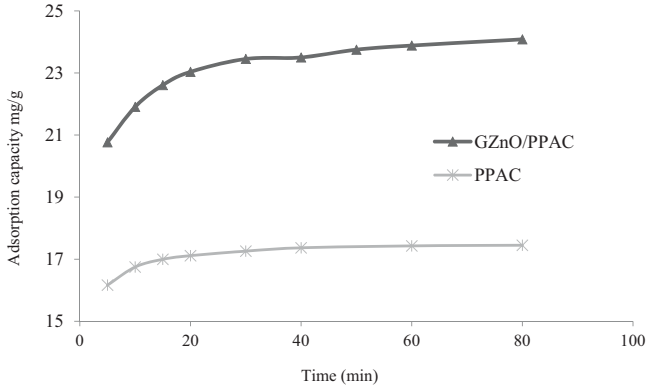

Fig. 8. Effect of contact time (pH = 2, Cr(VI) concentration = 50 mg/l, agitation speed = 200 rpm).

3.4. Effect of contact time on Cr(VI) adsorption

The influence of contact time on Cr(VI) adsorption by GZnO/AC and PPAC is depicted in Fig. 8. Based on the figure, the adsorp-

tion capacities of PPAC and GZnO/PPAC at 5 min were 16.16 and 20.76 mg/g, respectively. By increasing the contact time to 30 min, the adsorption capacities of the adsorbents changed to 17.25 and 23.34 mg/g, receptively. As the time proceeded to 80 min, a negligible change was seen in the adsorption capacities of theses adsorbents. From Fig. 8, it is obvious that adsorption capacity of GZnO/PPA increased sharply at first but, this was not significant for PPAC. Therefore, it can be concluded that the adsorption rate of Cr(VI) by GZnO/AC is higher than that of PPAC. The results also presented that the adsorption capacity of GZnO/AC was much higher than PPAC. Increase in adsorbent capacity with time can be attributed to more opportunity of contact between Cr(VI) and adsorption sites on the adsorbent surface (Khosravi et al., 2014). This can also due to the rapid saturation of available binding sites on the surface of the adsorbent (Pehlivan and Altun, 2008). The time needed to attain to equilibrium is important for determination of removal efficiency and estimation of feasibility and effectiveness of the adsorbent in the removal of different types of pollutants (Agarwal et al., 2006; Dakiky et al., 2002). Other studies have also showed the increase in removal efficiency with contact time increasing (Moussavi and Khosravi, 2011; Pehlivan and Altun, 2008; Sarin and Pant, 2006).

3.5. Effect of temperature on Cr(VI) adsorption

The influence of solution temperature on Cr(VI) removal is depicted in Fig. 9. The experimental data obviously showed that by increasing the solution temperature from 10 to 50 °C, the Cr(VI) removal percentage slightly changed from 93.25 to 97.81, respectively. This might be attributed to three reasons. 1; with the increase of temperature, the diffusion rate of Cr(VI) ions in the external mass transport process increases, 2; when the temperature is low, the kinetic energy of Cr(VI) is low and hence contact between the metal ions and the active sites of AC is insufficient, resulting in reduction of adsorption efficiency and three; temperature increase may also lead to the increase in number of adsorption sites as a result of breaking of some internal bonds near edge of active surface sites of adsorbent (Di Natale et al., 2015; Gottipati and Mishra, 2016). Although these reasons are not clear completely, but it can be generally stated that due to the increase of adsorption efficiency with temperature increase, the adsorption process is endothermic (Di Natale et al., 2015).

3.6. Kinetic study

Adsorption kinetic determines amount of mass transfer of adsorbate per time and determines adsorption rate. In this work, pseudo first and second order models were used. The linear forms of these equations are as below:

$$\frac{t}{q_t} = \frac{1}{k_2 q_e^2} + \frac{1}{q_e} t \tag{2}$$

$$\log(q_e - q_t) = \log q_e - \frac{k_1}{2.303} t \tag{3}$$

Where, qe and qt are amount of chromium adsorbed at equilibrium and at time t, respectively. K_1 and K_2 are pseudo first and pseudo second order rate constants (Bansal et al., 2009). The results of kinetic study are shown in Fig. 10, and their related parameters are represented in Table 1. Based on obtained data of adsorption kinetics, determination coefficient (R^2) value was higher for pseudo second order kinetic model, i.e it can be concluded that the experimental results fit better to second pseudo order model. Additionally, the qe value calculated from pseudo-second order was comparable to that obtained experimentally. As pseudo second order kinetic model is a chemosorption process, therefore, it can be concluded that adsorption of Cr(VI) on GZnO/PPAC is a chemical in nature (Duranoğlu et al., 2012; Yuan et al., 2009). Similarly, several researchers used pseudo second order model to show Cr(VI) adsorption on various activated carbons (Bayazit and Kerkez, 2014; Duranoğlu et al., 2012; Gottipati and Mishra, 2016; Sun et al., 2014; Yang et al., 2015). Parameters of adsorption kinetics are given in Table 1.

3.7. Adsorption isotherm study

For evaluation of GZnO/PPAC performance in the removal of Cr(VI) ions, isotherm studies were conducted. Isotherms models are important items for evaluation of an adsorbent behavior. Thus, Langmuir and Freundlich isotherm, as the most commonly models in adsorption studies, were used. The Langmuir isotherm assumes monolayer adsorption of a contaminant onto an adsorbent surface with a finite number of biding sites. it is generally known that the Langmuir isotherm is commonly used to monolayer, and the Freundlich isotherm to multilayer adsorption processes on heterogeneous surface (Sun et al., 2013). Langmuir model in linear form can be expressed as:

$$\text{Langmuir}: \frac{Ce}{qe} = \frac{1}{Kl * qmax} + \frac{C}{qmax} \tag{4}$$

Where, Ce is final Cr(VI) concentration (mg/l), qe is amount of Cr(VI) adsorbed (mg/g) and K_l (L/mg) is Langmuir constants related to energy of adsorption. The fundamental characteristics of the Langmuir equation can be described in terms of a dimensionless separation factor, RL, defined as:

$$RL = \frac{1}{1 + (qmax * KL)\,C0} \tag{5}$$

The RL values indicate the type of isotherm to be unfavorable (RL > 1), linear (RL = 1), favourable (0 < RL < 1) and irreversible (RL = 0) (23). Linear form of Freundlich isotherm model was used as Eq. (5):

$$\text{Freundlich}: \ln qe = \ln Kf + \frac{1}{n} \ln Ce \tag{6}$$

Where, Kf is maximum adsorption capacity (mg/g), and 1/n is the constant indicative of the intensity of the adsorption, n values between 1 and 10 represents beneficial adsorption. Fig. 11 shows the plotted models with related regression coefficients. The obtained isotherm parameters are given in Table 2. Higher determination coefficients (R^2) for Langmuir model in Fig. 11 and Table 2, suggest that adsorption of Cr(VI) on GZnO/PPAC follows Langmuir model better. Thus, it can be concluded that adsorption of Cr(VI) on GZnO/PPAC occurs on a monolayer phase and on a homogenous surface (Moussavi and Khosravi, 2010). Considering the Langmuir constant, adsorption energy of Cr(VI) on GZnO/PPAC was 1.089 l/mg. The RL values near to 0 in the Langmuir model demonstrates that the adsorption of Cr(VI) on these adsorbents is also favourable and irreversible (Table 2). Furthermore, as can be seen in Table 2, the value of n in Freundlich plot was between 1 and 10, representing good adsorption potential of GZnO/PPAC (Khosravi et al., 2014). The maximum adsorption capacity of GZnO/PPAC for Cr(VI) was 68.49 mg/g which was higher than those in the other studies (Table 3).

3.8. Thermodynamic study

The thermodynamic parameters determine whether the adsorption is spontaneous or not. Van't Hoff equation is used to estimate the thermodynamic parameters as following:

$$K_d = \frac{q_e}{C_e} \times \rho \tag{6}$$

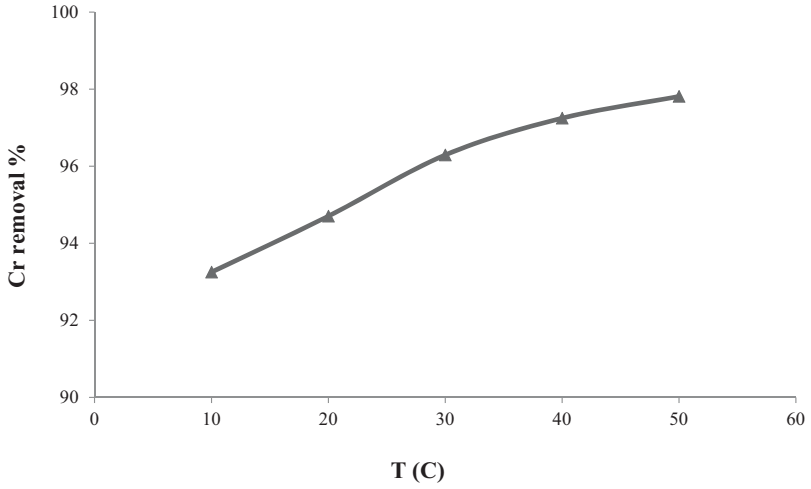

Fig. 9. Effect of solution temperature (pH = 2, Cr(VI) concentration = 50 mg/l, agitation speed = 200 rpm).

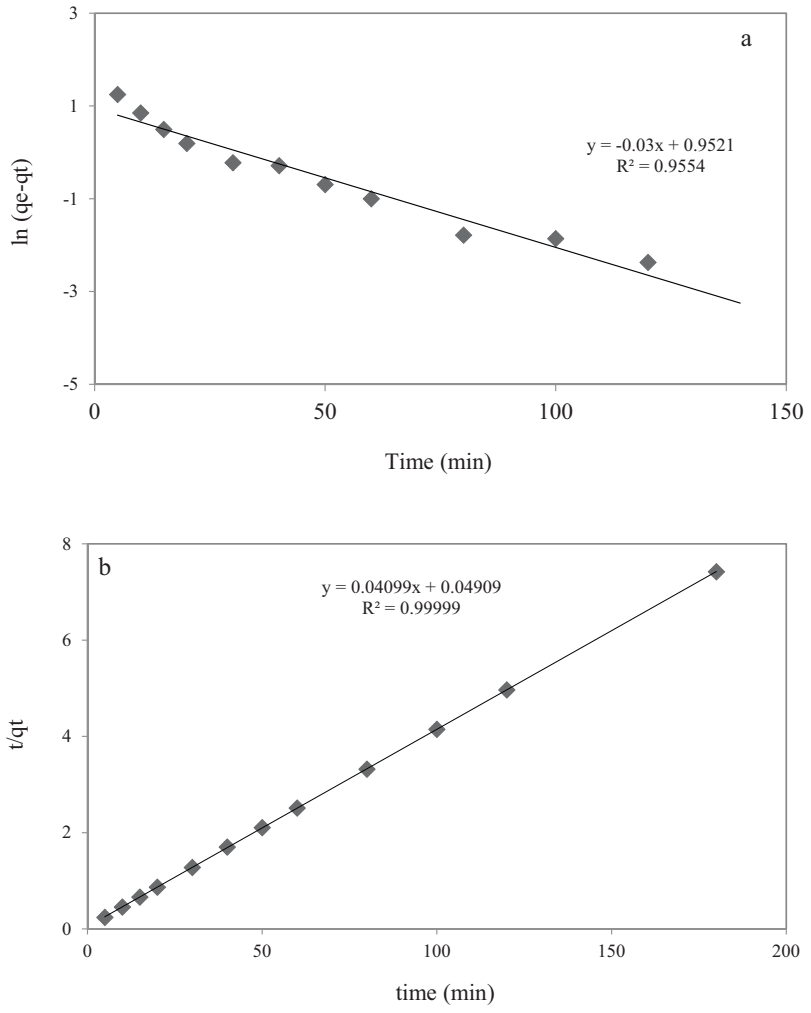

Fig. 10. Pseudo first order (a), and pseudo second order kinetics (b).

Table 1
Kinetic parameters of Cr(VI) adsorption.

Pseudo-first-order			Pseudo-second-order		
R^2	q_e (mg/g)	k_1	R^2	q_e (mg/g)	k_2
0.9554	2.59	0.03	0.99999	24.39	0.034

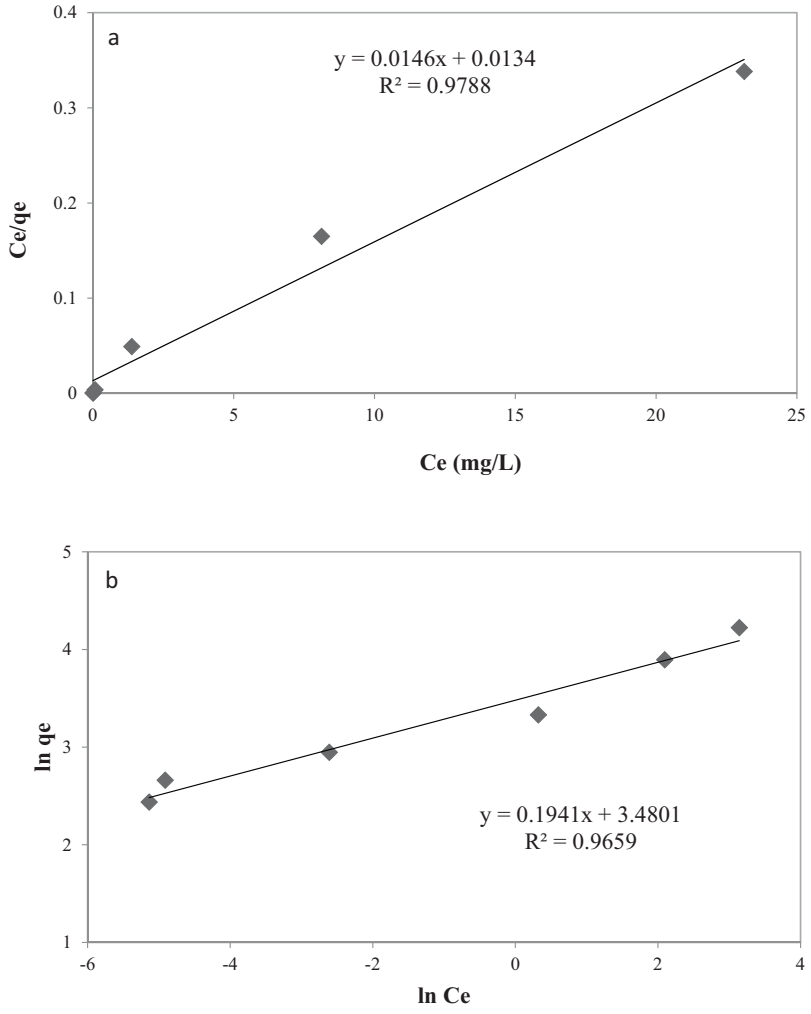

Fig. 11. Langmuir (a), Freundlich (b) plots for Cr(VI) adsorption on GZnO/PPAC.

Table 2
Isotherm constants for Cr(VI) adsorption on GZnO/PPAC.

Langmuir				Freundlich		
RL	R^2	qmax	KL	R2	KF	n
0.0003	0.978	68.49	1.089	0.965	6.396	1.847

Table 3
Comparison of adsorption capacity of GZnO/PPAC in this work with those obtained for different types of adsorbents from Langmuir model.

adsorbent	pH	Q max mg/g	References
magnetically modified multi-wall carbon nanotubes	1	14.28	[38]
magnetically modified activated carbon	1	5.07	[38]
activated carbon derived from acrylonitrileivinylbenzene	2	73.897	[37]
Microporous activated carbon	2	4.27	[24]
bamboo bark-based activated carbon	2	18.94	[27]
alumina/alginate (AlAlg) composite	2	17.45	[26]
dolomite	2	10.1	[42]
sawdust activated carbon	2	44.05	[43]
Low cost fertilizer industry waste material	2	15.24	[44]
granular Peganum Harmala seed	1.5	8.47	[23]
Powder of Peganum Harmala seed	1.5	18.18	[23]
GZnO/PPAC	2	68.49	This study

$$\Delta G^{\circ} = -RTLnK_d \quad (7)$$

$$LnK_d = \frac{\Delta S^{\circ}}{R} - \frac{\Delta H^{\circ}}{RT} \quad (8)$$

Where, Kd is thermodynamic equilibrium constant, (ΔH°) is enthalpy change, (ΔS°) is entropy change, ρ is the solution density (ρ= 1000 g/L), R and T represent the universal gas constant (8.314 J/mol K) and the system temperature (K). The values of ΔS°

Table 4
Thermodynamic parameters for Cr(VI) adsorption by GZnO/PPAC.

T (K)	ΔH° (kJ/mol)	ΔS° (J/mol K)	ΔG° (kJ/mol)
283	23.035	154.68	−20.8
293			−22.16
303			−25.45
313			−23.86
323			−26.89

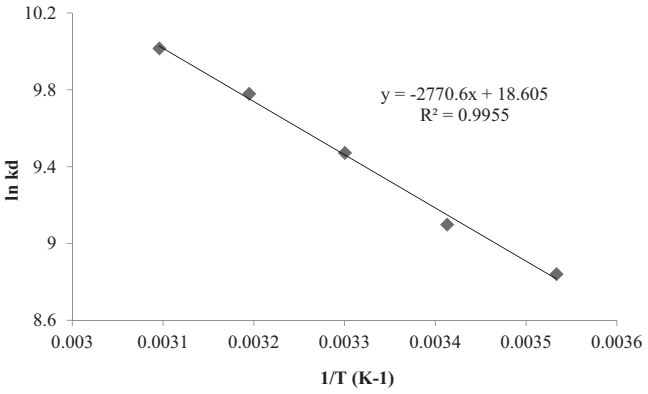

Fig. 12. Van't Hoff plot for Cr(VI) adsorption onto PPAC.

(J/mol K) and ΔH° (KJ/mol) are determined from the intercept and slope of liner plots of Ln(Kd) versus 1/T. Thermodynamic data obtained for 200 mg/l Cr(VI) concentration at pH 2 are given in Table 2. The negative values of ΔG° (Table 4) indicate that the adsorption process was favourable and spontaneous in nature. Furthermore, the negative sign of ΔG° value with an increase of temperature suggests the adsorption is more favourable at higher temperature. Moreover, if ΔH° < 40 KJ/mol, according to literature, it can be stated that the physical adsorption occurs (Yao et al., 2010). While in the case of ΔH° > 29 KJ/mol, chemosorption can occur. The amount of enthalpy change in the present study was 23 kj/mol for GZnO/PPAC, showing a physical adsorption process. Complexation reaction can also occur. Moreover, the positive value of ΔS° in this study confirms the feasibility of adsorption and the increased randomness at the sorbent-solution interface during Cr(VI) adsorption onto GZnO/PPAC (Nityanandi and Subbhuraam, 2009). Chemical adsorption is responsible for adsorption if the enthalpy change is >29 KJ/mol, and that of complexation is between 8 and 60 kJ/mol (Duranoğlu et al., 2012) (Fig. 12).

4. Conclusion

A new type of powdered activated carbon was produced by use of ultrasonic waves as activator agent. BET and FESEM analyses showed that the synthesized activated carbon has a high surface area and porosity. In the present work, a novel and eco-friendly method, green synthesis, was used for the synthesis of zinc oxide NPs. Extract of *Peganum harmala* seed was used as stabilizing and coating agent for NPs synthesis. FTIR spectrum confirmed that polyphenolic compounds and proteins have an essential role in the synthesis of NPs. Moreover, TEM images presented a size of 40 nm for the NPs. The analysis showed a layer of capping materials of plant extract on the NPs. Green NPs of zinc oxide (GZnO) was coated onto activated carbon and examined for the feasibility of Cr(VI) removal from aqueous solution. In addition, EDAX analysis indicated presence of NPs on the surface of activated carbon. Based on the results, the Cr(VI) removal efficiency of GZnO/PPAC was much higher than that of PPAC due to the presence of NPs on GZnO/PPAC. The results also showed that the removal percentage of Cr(VI) was strongly dependent on pH values. Cr(VI) adsorption onto GZnO/PPAC was endothermic in nature and thus, increased with increase in temperature. Furthermore, thermodynamic study of Cr(VI) adsorption on GZnO/PPAC presented a negative value of free gibbes energy (ΔG°), indicating a spontaneous reaction. ΔH° value was positive showing the reaction was endothermic. Experimental data fitted well with the pseudo second order model, indicating chemisorption. The results of equilibrium study showed that obtained data exhibited better fit to Langmuir isotherm, indicating that the surface of the adsorbent is homogenous and thus, monolayer adsorption occurs. Generally, ultrasonic wave in the present study has been shown to be an effective activator for production of activated carbon. Moreover, extract of *Peganum harmala* seed was an efficient candidate for the synthesis of GZnO NPs. The results also showed that the new synthesized adsorbent had a high adsorption capacity, 68.49 mg/g, for Cr(VI) removal from aqueous solutions.

Acknowledgement

The authors are grateful for financial support of Ardabil University of Medical Sciences for this research work.

References

APHA, AWWA, WEF, 2005. standard Methods for the Examination of Water and Wastewater, 20 ed., American Public Health Association Washington, DC.
Agarwal, G.S., Bhuptawat, H.K., Chaudhari, S., 2006. Biosorption of aqueous chromium(VI) by Tamarindus indica seeds. Bioresour. Technol. 97, 949–956.
Agnieszka, G.-P., Marek, M., Stanisław, P., Dariusz, S., 2011. Simultaneous adsorption of chromium(VI) and phenol on natural red clay modified by HDTMA. Chem. Eng. J.
Ahmad, B.A., Mangwandi, C., Ala'a, H.A.-M., Gavin, M.W., Stephen, J.A., Mohammad, N.M.A., 2011. Kinetic and thermodynamics of chromium ions adsorption onto low-cost dolomite adsorbent. Chem. Eng. J.
Babak, K., Roshanak, R.K., Mahdi, F., Amir Hossein, M., Ali, E., Ali, A., Ahmad Reza, Y., Allah Bakhsh, J., 2014. Enhanced chromium (VI) removal using activated carbon modified by zero valent iron and silver bimetallic nanoparticles. J. Environ. Health Sci. Eng. 115.
Bansal, M., Singh, D., Garg, V.K., 2009. A comparative study for the removal of hexavalent chromium from aqueous solution by agriculture wastes' carbons. J. Hazard. Mater. 171, 83–92.
Bayat, B., 2002. Comparative study of adsorption properties of Turkish fly ashes. II. The case of chromium (VI) and cadmium (II). J. Hazard. Mater. 95, 275–290.
Bayazit, Ş.S., Kerkez, Ö., 2014. Hexavalent chromium adsorption on superparamagnetic multi-wall carbon nanotubes and activated carbon composites. Chem. Eng. Res. Des. 92, 2725–2733.
Dakiky, M., Khamis, M., Manassra, A., Mer'eb, M., 2002. Selective adsorption of chromium(VI) in industrial wastewater using low-cost abundantly available adsorbents. Adv. Environ. Res. 6, 533–540.
Di Natale, F., Erto, A., Lancia, A., Musmarra, D., 2015. Equilibrium and dynamic study on hexavalent chromium adsorption onto activated carbon. J. Hazard. Mater. 281, 47–55.
Duranoğlu, D., Trochimczuk, A.W., Beker, U., 2012. Kinetics and thermodynamics of hexavalent chromium adsorption onto activated carbon derived from acrylonitrile-divinylbenzene copolymer. Chem. Eng. J. 187, 193–202.
Fazlzadeh, M., Abdoallahzadeh, H., Khosravi, R., Alizadeh, B., 2016. Removal of acid black 1 from aqueous solutions using Fe_3O_4 magnetic nanoparticles. J. Mazandaran Univ. Med. Sci. 26, 174–186.
Fazlzadeh, M., Rahmani, K., Zarei, A., Abdoallahzadeh, H., Nasiri, F., Khosravi, R., 2017. A novel green synthesis of zero valent iron nanoparticles (NZVI) using three plant extracts and their efficient application for removal of Cr(VI) from aqueous solutions. Adv. Powder Technol. 28, 122–130.
Ghaedia, M., Sadeghiana, B., Amiri Pebdania, A., Sahraeib, R., Daneshfarb, A., Duranc, C., 2012. Kinetics, thermodynamics and equilibrium evaluation of direct yellow 12 removal by adsorption onto silver nanoparticles loaded activated carbon. Chem. Eng. J. 187, 13341.
Gopalakannan, V., Periyasamy, S., Viswanathan, N., 2016. One pot eco-friendly synthesis of highly dispersed alumina supported alginate biocomposite for efficient chromium(VI) removal. J. Water Process Eng. 10, 113–119.
Gottipati, R., Mishra, S., 2016. Preparation of microporous activated carbon from Aegle Marmelos fruit shell and its application in removal of chromium(VI) from aqueous phase. J. Ind. Eng. Chem. 36, 355–363.
Granados-Correa, F., Jiménez-Becerril, J., 2009. Chromium (VI) adsorption on boehmite. J. Hazard. Mater. 162, 1178–1184.
Huang, L., Weng, X., Chen, Z., Megharaj, M., Naidu, R., 2014. Green synthesis of iron nanoparticles by various tea extracts: comparative study of the reactivity. Spectrochim. Acta A 130, 295–301.
Jing, J.P., Jun, J., Ren, K.X., 2014. Removal of Cr(VI) from aqueous solutions by Na_2SO_3/$FeSO_4$ combined with peanut straw biochar. Chemosphere 101, 71–76.

Jung, C., Heo, J., Han, J., Her, N., Lee, S.-J., Oh, J., Ryu, J., Yoon, Y., 2013. Hexavalent chromium removal by various adsorbents: powdered activated carbon, chitosan, and single/multi-walled carbon nanotubes. Sep. Purif. Technol. 106, 63–71.

Khosravi, R., Fazlzadehdavil, M., Barikbin, B., Taghizadeh, A.A., 2014. Removal of hexavalent chromium from aqueous solution by granular and powdered Peganum Harmala. Appl. Surf. Sci. 292, 670–677.

Limei, W., Libing, L., Guocheng, L., Faxiang, Q., Yujuan, H., Xiaoyu, W., 2013. Micro-electrolysis of Cr (VI) in the nanoscale zero-valent iron loaded activated carbon. J. Hazard. Mater. 254–255, 277–283.

Liu, Q.-S., Zheng, T., Wang, P., Guo, L., 2010. Preparation and characterization of activated carbon from bamboo by microwave-induced phosphoric acid activation. Ind. Crops Prod. 31, 233–238.

Machado, S., Stawiński, W., Slonina, P., Pinto, A.R., Grosso, J.P., Nouws, H.P.A., Albergaria, J.T., Delerue-Matos, C., 2013. Application of green zero-valent iron nanoparticles to the remediation of soils contaminated with ibuprofen. Sci. Total Environ. 461–462, 323–329.

Mahmood-ul-Hassan, M., Vishandas, S., Ejaz, R., Muhammad, Y., 2015. Removal of Cd, Cr, and Pb from aqueous solution by unmodified and modified agricultural wastes.

Mehrorang, G., Maryam, G., Syamak, N.K., Reza, S., Ali, D., 2013. Palladium, silver, and zinc oxide nanoparticles loaded on activated carbon as adsorbent for removal of bromophenol red from aqueous solution. J. Ind. Eng. Chem. 19, 1209–1217.

Moussavi, G., Khosravi, R., 2010. Removal of cyanide from wastewater by adsorption onto pistachio hull wastes: parametric experiments, kinetics and equilibrium analysis. J. Hazard. Mater. 183, 724–730.

Moussavi, G., Khosravi, R., 2011. The removal of cationic dyes from aqueous solutions by adsorption onto pistachio hull waste. Chem. Eng. Res. Des. 89, 2182–2189.

Nethaji, S., Sivasamy, A., Mandal, A.B., 2013. Preparation and characterization of corn cob activated carbon coated with nano-sized magnetite particles for the removal of Cr(VI). Bioresour. Technol. 137, 94–100.

Nityanandi, D., Subbhuraam, C.V., 2009. Kinetics and thermodynamic of adsorption of chromium(VI) from aqueous solution using puresorbe. J. Hazard. Mater. 170, 876–882.

Pehlivan, E., Altun, T.r., 2008. Biosorption of chromium(VI) ion from aqueous solutions using walnut, hazelnut and almond shell. J. Hazard. Mater. 155, 378–384.

Pirsaheb, M., Dargahi, A., Hazrati, S., Fazlzadehdavil, M., 2014. Removal of diazinon and 2, 4-dichlorophenoxyacetic acid (2, 4-D) from aqueous solutions by granular-activated carbon. Desalin. Water Treat. 52, 4350–4355.

Prasad, K.S., Gandhi, P., Selvaraj, K., 2014. Synthesis of green nano iron particles (GnIP) and their application in adsorptive removal of As(III) and As(V) from aqueous solution. Appl. Surf. Sci. 317, 1052–1059.

Ramesh, M., Anbuvannan, M., Viruthagiri, G., 2015. Green synthesis of ZnO nanoparticles using Solanum nigrum leaf extract and their antibacterial activity. Spectrochim. Acta A 136, 864–870 (Part B).

Sarin, V., Pant, K.K., 2006. Removal of chromium from industrial waste by using eucalyptus bark. Bioresour. Technol. 97, 15–20.

Shahwan, T., Abu Sirriah, S., Nairat, M., Boyacı, E., Eroğlu, A.E., Scott, T.B., Hallam, K.R., 2011. Green synthesis of iron nanoparticles and their application as a Fenton-like catalyst for the degradation of aqueous cationic and anionic dyes. Chem. Eng. J. 172, 258–266.

Sun, Y., Yue, Q., Gao, B., Gao, Y., Li, Q., Wang, Y., 2013. Adsorption of hexavalent chromium on Arundo donax Linn activated carbon amine-crosslinked copolymer. Chem. Eng. J. 217, 240–247.

Sun, Y., Yue, Q., Mao, Y., Gao, B., Gao, Y., Huang, L., 2014. Enhanced adsorption of chromium onto activated carbon by microwave-assisted H3PO4 mixed with Fe/Al/Mn activation. J. Hazard. Mater. 265, 191–200.

Vinod, K.G., Arshi, R., Arunima, N., 2010. Adsorption studies on the removal of hexavalent chromium from aqueous solution using a low cost fertilizer industry waste material. J. Colloid Interface Sci. 342, 135–141.

Wang, T., Lin, J., Chen, Z., Megharaj, M., Naidu, R., 2014. Green synthesized iron nanoparticles by green tea and eucalyptus leaves extracts used for removal of nitrate in aqueous solution. J. Clean. Prod. 83, 413–419.

Weng, X., Huang, L., Chen, Z., Megharaj, M., Naidu, R., 2013. Synthesis of iron-based nanoparticles by green tea extract and their degradation of malachite. Ind. Crops Prod. 51, 342–347.

Yang, J., Yu, M., Chen, W., 2015. Adsorption of hexavalent chromium from aqueous solution by activated carbon prepared from longan seed: kinetics, equilibrium and thermodynamics. J. Ind. Eng. Chem. 21, 414–422.

Yao, Y., Xu, F., Chen, M., Xu, Z., Zhu, Z., 2010. Adsorption behavior of methylene blue on carbon nanotubes. Bioresour. Technol. 101, 3040–3046.

Yuan, P., Fan, M., Yang, D., He, H., Liu, D., Yuan, A., Zhu, J., Chen, T., 2009. Montmorillonite-supported magnetite nanoparticles for the removal of hexavalent chromium [Cr(VI)] from aqueous solutions. J. Hazard. Mater. 166, 821–829.

Zhang, Y.-J., Ou, J.-L., Duan, Z.-K., Xing, Z.-J., Wang, Y., 2015. Adsorption of Cr(VI) on bamboo bark-based activated carbon in the absence and presence of humic acid. Colloids Surf. A 481, 108–116.

Zhongren, Y., Samantha, E.B., Jinwen, W., James, E., 2009. Removal of chromium Cr(VI) by low-cost chemically activated carbon materials from water. J. Hazard. Mater. 166, 74–78.